Chapter 7 THERMAL INFRARED

The above chapters largely describe the nature of data observed via reflected sunlight. Data from such systems have one obvious problem - they don't work well at night. This leads fairly promptly to a desire to work in the portion of the electromagnetic spectrum defined by the thermal emission intrinsic to all objects at a temperature above absolute zero. There are more subtle motivations, as well, because one can extract information from thermal imagery which is not available in the reflective domain - notably temperature.

A IR basics

Reflected vs. emitted radiation - in the visible, we mostly see by reflected (sun-light). In the IR, there is a reflected solar component (during the day), but much of the remote sensing is due to emitted IR, particularly in the mid-IR range (5 microns). Figure 2-9 in chapter 2 shows how the location of the peak in the spectrum and the amplitude of the radiation change with temperature. As a consequence of these curves, we can both 'see' in the ir, and obtain temperature measurements of remotely sensed scenes.

1 Stefan-Boltzman Law

We saw the Stefan-Boltzman law earlier in the text, and briefly repeat some elements here. Of particular interest is the difference between the sun as a black-body, and terrestrial objects.

Figure 7-1.
If you look at the radiation from the sun, the sun acts like a blackbody at about 6000 K. Of course, the radiation from the sun decreases as per the inverse square law, and the incident radiation observed at the earth is decreased by that factor: $\left(radius_{sun}/radius_{earth\ orbit}\right)^2$.
As a consequence, if you look at the 3-5 micron wavelength range, it is right in the middle of the transition region from dominance by reflected solar radiation to dominance by emitted thermal radiation for terrestrial targets.

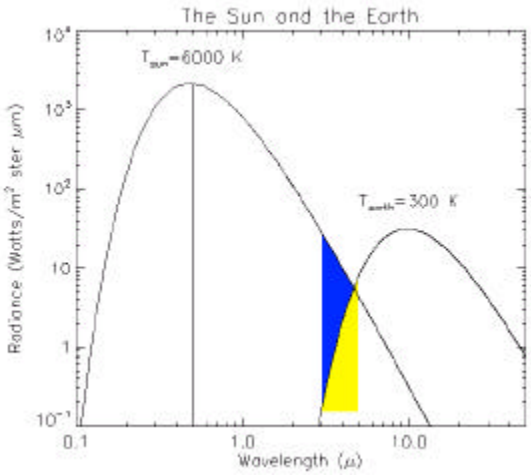

Two laws define the shapes shown in the upper figure.

2 Wien's displacement law

Wien's displacement law says that the wavelength of the peak is inversely related to the temperature:

$$\lambda_m = \frac{a}{T} \qquad \text{(Eqn. 7.1)}$$

where a is a constant: $a = 2898\ \mu m/K$.

3 Stefan-Boltzmann: Radiance aT^4

The Stefan-Boltzmann law defines the total power:

$$S = \sigma T^4, \qquad \text{(Eqn. 7.2)}$$

where σ is again a constant: $\sigma = 5.669 \times 10^{-8}$ W m^{-2} K^{-4}.

4 Emissivity

The above numbers are for so-called 'black-bodies', which are perfect absorbers and emitters of radiation. Real objects all have an emissivity (ε) which is between 0 and 1, and modifies the emitted power, S - *power* $= \varepsilon \sigma T^4$. The table below shows some average values for the 8-12 micron wavelength range. Just as with reflective spectra, there are fine scale variations in the emissivity, which are unique to the materials.

Material	Emissivity
Granite	0.815
Sand, quartz, large-grain	0.914
Asphalt, paving	0.959
Concrete walkway	0.966
water, with thin layer of petroleum	0.972
Water, pure	0.993

Table 1. From Sabins, ***Remote Sensing and Image Interpretation***, page 138.
His citation: Buettner and Kern, JGR, 70, p1333, 1965.

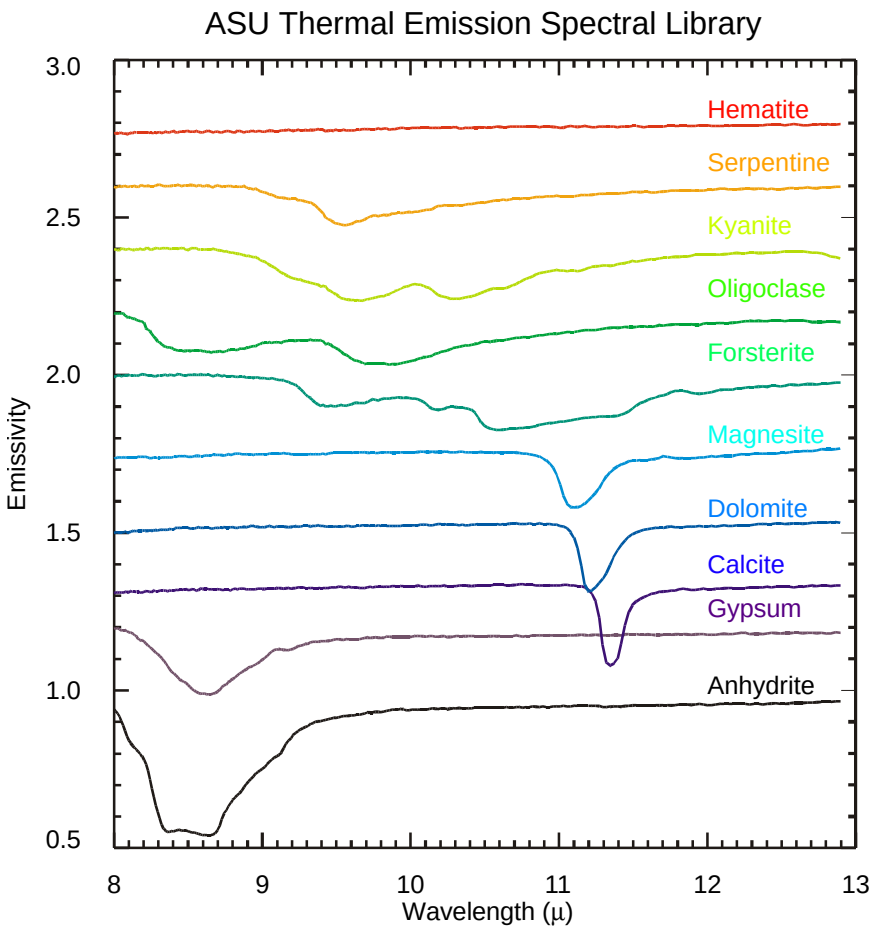

Figure 7.2 Minerals have a number of interesting spectral characteristics that make the thermal IR region interesting for geological work. This figure is a "stack-plot" - the curves here are offset by a constant value of 0.2. Most of these materials have an emissivity near 1 at the high wavelength limit (13 μ). Notice how the variation in emissivity is fairly modest, in contrast for the much larger variation seen in the reflective bands (figures 5.1 and 5.2).

5 Atmospheric Absorption

In the infrared wavelength range, atmospheric absorption, due primarily to water (H_2O) and carbon dioxide (CO_2), becomes a very important consideration. (Figure 3.15)

B More IR

1 Kinetic Temperature

Resuming now with newer material, the concept of kinetic temperature appears. A remote sensing instrument, in general, will not be able to factor emissivity into the image analysis. As a result, although the radiated quantity is $\varepsilon\sigma\, T_{kinetic}^4$, the sensor data must be interpreted as $\sigma\, T_{radiated}^4$. Here, $T_{kinetic}$ is the "real" temperature, meaning the temperature one would measure with a thermometer at the target. Setting the two equal, we obtain: $s\, T_{radiated}^4 = e s\, T_{kinetic}^4$, or $T_{radiated}^4 = e T_{kinetic}^4$. Note that ε is a number less than one, so $T_{kinetic} > T_{radiated}$ by a factor which is just the fourth root of ε, or

$T_{radiated} = \sqrt[4]{e}\ T_{kinetic}$

2 Thermal inertia, conductivity, capacity, diffusivity

Normal reflective observations depend primarily on the instantaneous values for the incident radiation, but thermal IR observations are very much dependent on the thermal history of the target region.
See: Physical Principles of Remote Sensing, W. G. Rees, p109-113

a Thermal Conductivity

Thermal Conductivity is the rate at which heat will pass through a material. It is measured as the amount of heat (calories) flowing through a cross-section area (cm^2), over a set distance (thickness in cm), at a given temperature difference (^oC). It is given the symbol:
$K\left(\frac{\text{calories}}{\text{cm s }^\circ\text{C}}\right)$, where the nominal value for rocks is 0.006 in these peculiar units. (compare water, ~0.001). Rocks are generally poor conductors of heat compared to metals, but are better than loose soil, which tends to have insulating air pockets.

b Thermal Capacity

Thermal Heat Capacity is a measure of the increase in thermal energy content (heat) per degree of temperature rise. It is measured as the number of calories required to rais the temperature of 1 gm of material by 1 ^oC. It is given the symbol: $C\left(\frac{\text{calories}}{cm^3\ ^\circ\text{C}}\right)$
The specific heat is a closely related quantity, modifed by the mass density:
$c\left(\frac{\text{calories}}{gm\ ^\circ\text{C}}\right)$ where the value for water is very high (1.0), about 5 times that for rocks.

(Note: $C = r\ c$, where ρ is the mass density in $\frac{gm}{cm^3}$)

c Inertia

Thermal Inertia is the resistance of a material to temperature change, indicated by the time dependent variations in temperature during a full heating/cooling cycle.
$P = \sqrt{K\ r\ c}\left(\frac{\text{calories}}{\text{cm}^2\ ^\circ\text{C}\ \text{s}^{\frac{1}{2}}}\right)$ varies by a factor of 4 or 5 for the range of materials shown in figure 5-5 of Sabins.

d Thermal Diffusivity

Thermal diffusivity is a measure of the rate of internal heat transfer within a substance. IT is related to the conductivity: $k = \frac{K}{c\ r}\ \left(\text{cm}^2/\text{s}\right)$. In remote sensing, it relates the ability of a substance to transfer heat from the surface to the subsurface during the day (heating period), and from the subsurface to the surface during the night (cooling period).

	Water	Sandy Soil	Basalt	Stainless Steel
K	0.0014	0.0014	0.0050	0.030
C	1.0	0.24	0.20	0.12
ρ	1.0	1.82	2.80	7.83
P	0.038	0.024	0.053	0.168

Table 2. From the remote sensing tutorial, http://eerst.gsfc.nasa.gov/Sect9/Sect9_3.html. Units are cgs. See also table 6-4 in Avery and Berlin, page 123.

e Diurnal Temperature Variation:

The net result, and important when interpreting images.

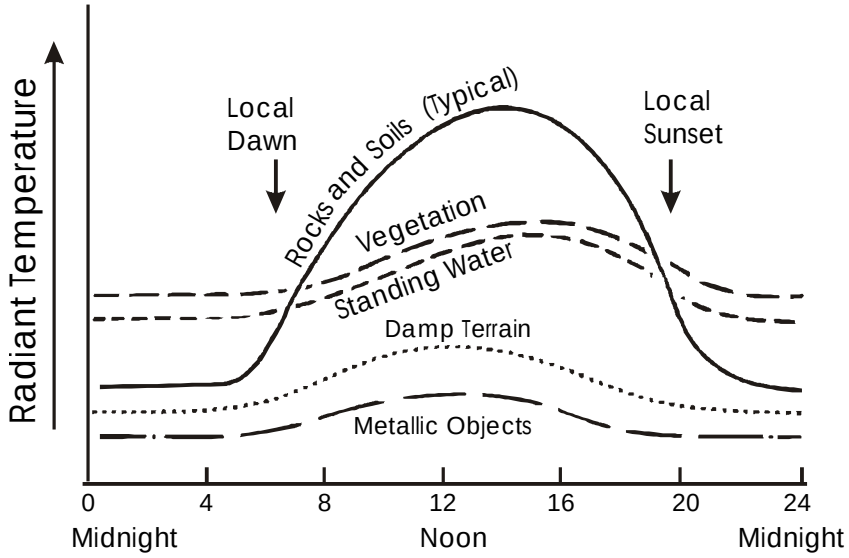

Figure 7.3 Thermal inertia. Note the times of thermal "cross-over", where the rocks and vegetation have the same temperature. At such times, it will be difficult to distinguish such scene elements.

C LANDSAT

Infrared data from Landsat were shown in Chapter 1 for a San Diego scene. Here, a second example is shown where the Landsat 7 thermal band is used. The illustration is from over northern Greenland, at Thule AFB. In the color picture below, the 60-meter resolution data from Band 6 was resampled using cubic convolution to an effective pixel size of 5 meters. This was then combined with panchromatic band data into a Red-Green Blue picture below. Band 6 data are shown in red and the panchromatic band data are assigned to both the green and blue channels.

Note how some features are shown to be warmer than the surrounding snow due to heating from the 24-hour sunlight now being experienced at this high northern latitude. The runway and various buildings on the base show relative warmth. The southern sides of the storage tanks near the base show somewhat greater warmth than the northern sides. Exposed rock on the hillsides to the north are emitting greater thermal radiation than the snow.

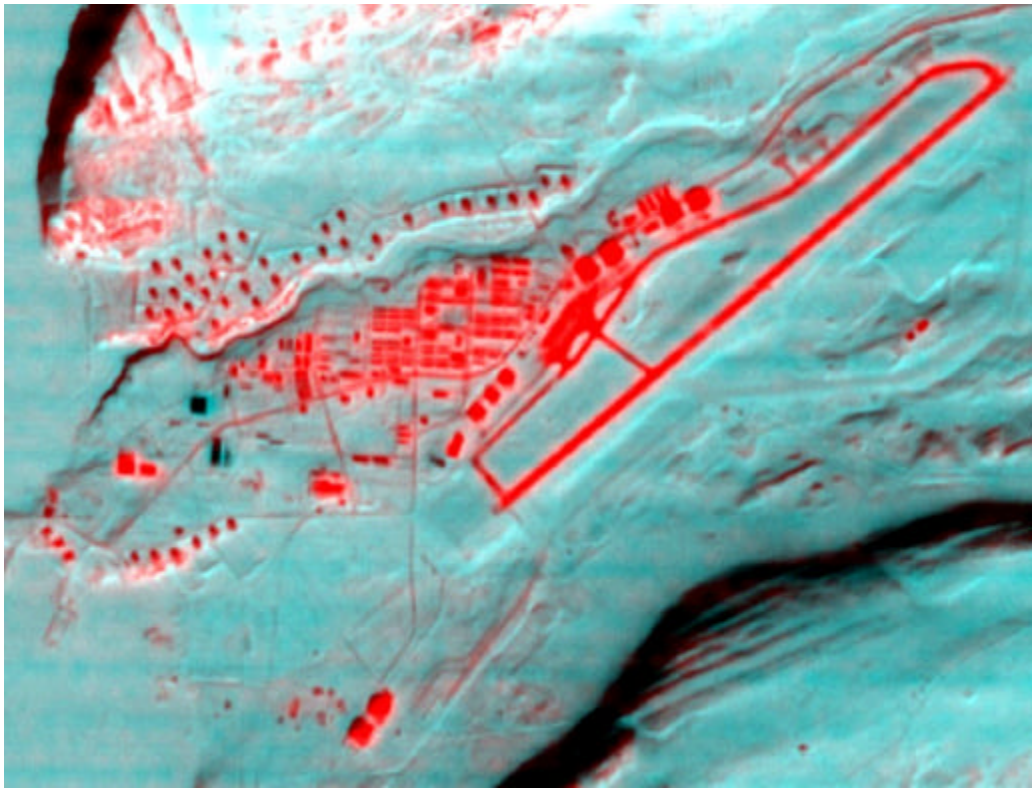

Figure 7-4. (Jim Storey of the EROS Data Center did the resampling and enhancement of this image, as part of the Landsat 7 calibration effort.)

D FLIR

Military airborne systems - see Recon-optical.

E Early Weather Satellites

Weather satellites are some of the primary IR platforms. Historically, the first were small polar orbiting platforms (TIROS, NIMBUS), followed by the first geosycnchronous platforms (ATS). The first illustrations here are in the visible wavelengths. These can be considered additional perspective on the question: can surveillance be done a the tactical or strategic level from high altitudes.

1 TIROS

The Television Infrared Observation Satellite (TIROS) was the first series of meteorological satellites to carry television cameras to photograph the Earth's cloud cover and demonstrate the value of using spacecraft for meteorological research and weather forecasting. The first TIROS was launched on 1 April 1960 and returned 22952 cloud cover photos. The satellite was tiny by modern standards: Mass: 120 kg. Perigee: 656 km. Apogee: 696 km. Inclination: 48.4 deg. RCA built the small cylindrical vehicle: 42" in diameter, 19" in height

TIROS has a complicated history of name changes and aliases, sensor packages, and other parameters. Between 1960 and 1965 ten TIROS satellites were launched. They were 18-sided cylinders covered on the sides and top by solar cells, with openings for two TV cameras on opposite sides. Each camera could acquire 16 images per orbit at 128 second intervals.

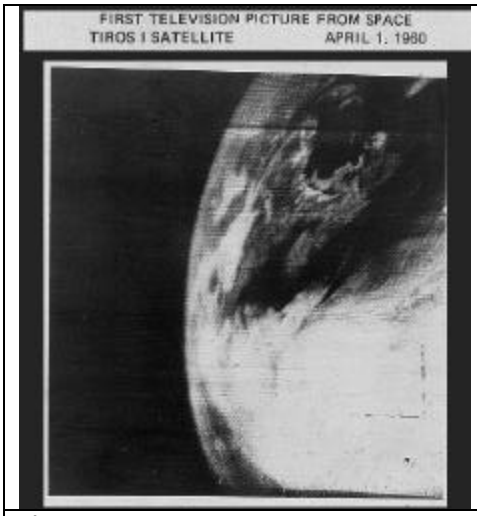

a) TIROS

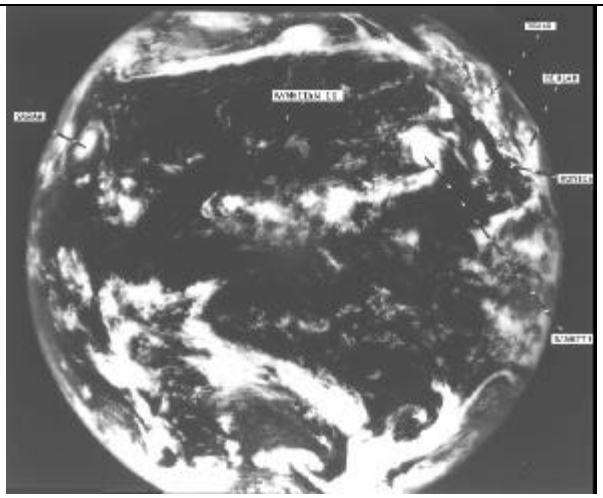

b) ATS

Figure 7-5.

2 NIMBUS

Nimbus, a second-generation meteorological satellite, named for a cloud formation, was larger and more complex than the TIROS satellites. Nimbus 1 was launched on 28 August 1964 and carried two television cameras and two infrared cameras. Nimbus 1 had only about a one-month life span; six more missions were launched, with Nimbus 7 operating from 1978 through 1993.

The polar-orbiting spacecraft consisted of three major elements: (1) a sensory ring, (2) solar paddles, and (3) the control system housing. The solar paddles and the control system housing were connected to the sensory ring by a truss structure, giving the satellite the appearance of an ocean buoy. Nimbus, depending on the experiments carried, was 3.04 to 3.7 m tall, 1.52 m in diameter at the base, and 3 to 3.96 m across with solar paddles extended.

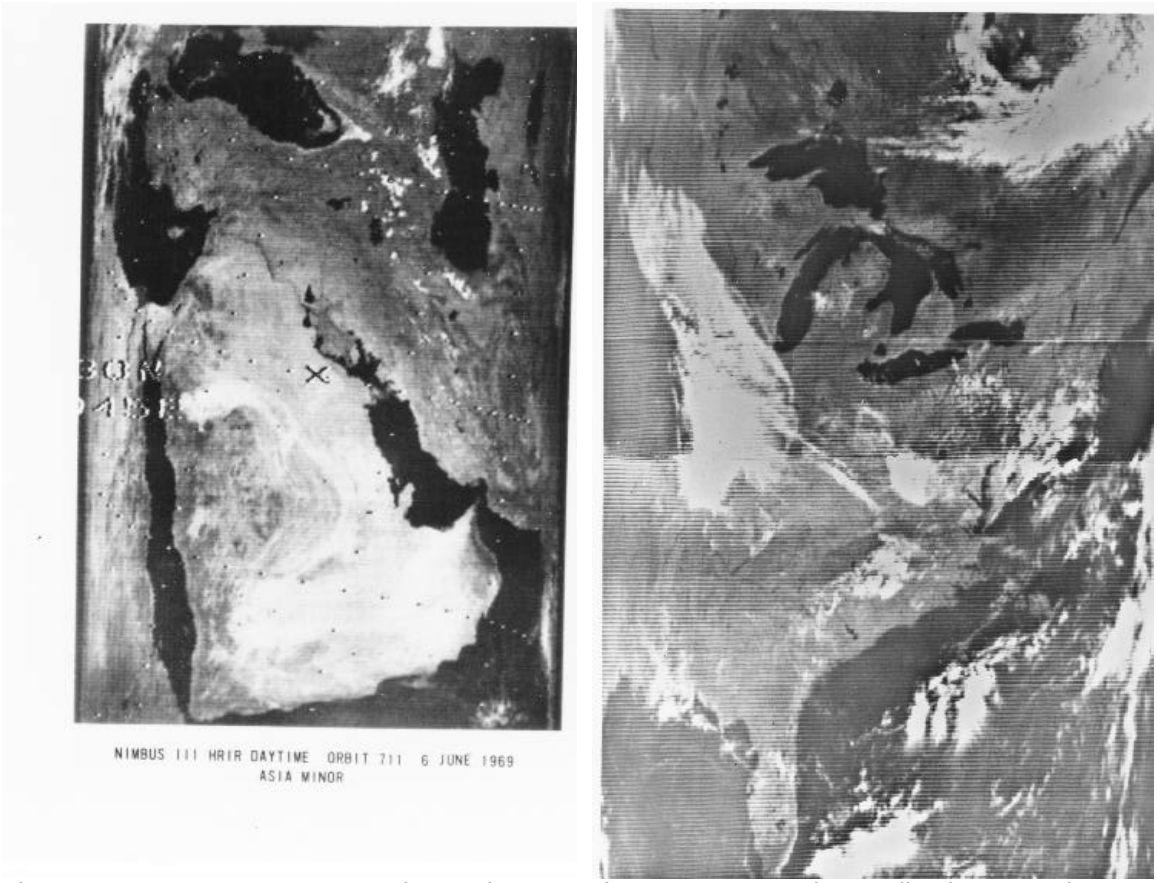

Figure 7-6 NIMBUS 1 Mass: 376 kg. Perigee: 429 km. Apogee: 937 km. Inclination: 98.7 deg. Returned 27,000 cloud cover images.

The spacecraft carried an advanced vidicon camera system for recording and storing remote cloudcover pictures, an automatic picture transmission camera for providing real-time cloud cover pictures, and a high-resolution infrared radiometer (3.4 to 4.2 micron) to complement the daytime TV coverage and to measure nighttime radiative temperatures of cloud tops and surface terrain.

3 Applied Technology Satellites (ATS)

The Applied Technology Satellite (ATS) series of satellites were designed to be geosynchronous orbiters, and were primarily communications technology testbeds. Several carried weather packages, however, and were precursors to today's GOES satellites.

a ATS-1

ATS-1 was launched in 1966. During its 18-year lifetime, ATS-1 examined spin stabilization techniques, investigated the geostationary environment, and performed several communications experiments. Its VHF experiment tested the ability to act as a link between ground stations and aircraft, demonstrated collection of meteorological data from remote terminals, and evaluated the feasibility of using VHF signals for navigation. The mission also provided the first full-Earth cloud cover images.

b ATS-3

ATS-3 was built by the Space Systems Division of Hughes Aircraft, El Segundo, CA. It was nearly identical to ATS-1. (ATS2 & 4 both failed to orbit properly.) The satellite was launched from NASA's Cape Kennedy on November 5, 1967, on top of an Atlas-Agena D launch vehicle. The satellite was initially placed in geosynchronous orbit at 47° West longitude, and was moved to several other locations to support various experiments before running out of fuel at 105° West longitude. The satellite remained in operation as a communications satellite for over 25 years.

Satellite Characteristics: THESE NUMBERS NEED SERIOUS CHECKING - look at GSFC

	ATS-1	ATS-3
Mass	295 kg. ?	352 kg.
Diameter	57.6" 1.42 m	57.6" 1.8 m
Height	54" 1.35 m	54" 1.42 m
Stabilization	Spin	Spin
Wavelength	0.475μm-0.630μm	0.39μm - 0.70μm
Spatial Resolution	>4km @ satellite subpoint	
Swath (Scan Angle): FOV	$15° \times 15°$	

Solar array providing 180W BOL, 2 6 Ah NiCd batteries,

c Spin Scan Cloud Cover Camera (SSCC)

The SSCC consisted of a 2-element Cassegrain-type telescope. Light entering the system was reflected from a 13.7cm diameter, 25.4cm focal length primary parabolic mirror onto a flat secondary quartz mirror to produce an image on the face of an aperture plate. The light was then passed through the 0.025mm diameter aperture and haze filter to impinge onto a photocathode backed by a photomultiplier tube. The entire assembly could be stepped ±7.5° to produce a N-S scan corresponding to 52° north and south latitude. It took 20 minutes to scan one scene.

The first full color picture at high enough altitude to see the full disk of the Earth

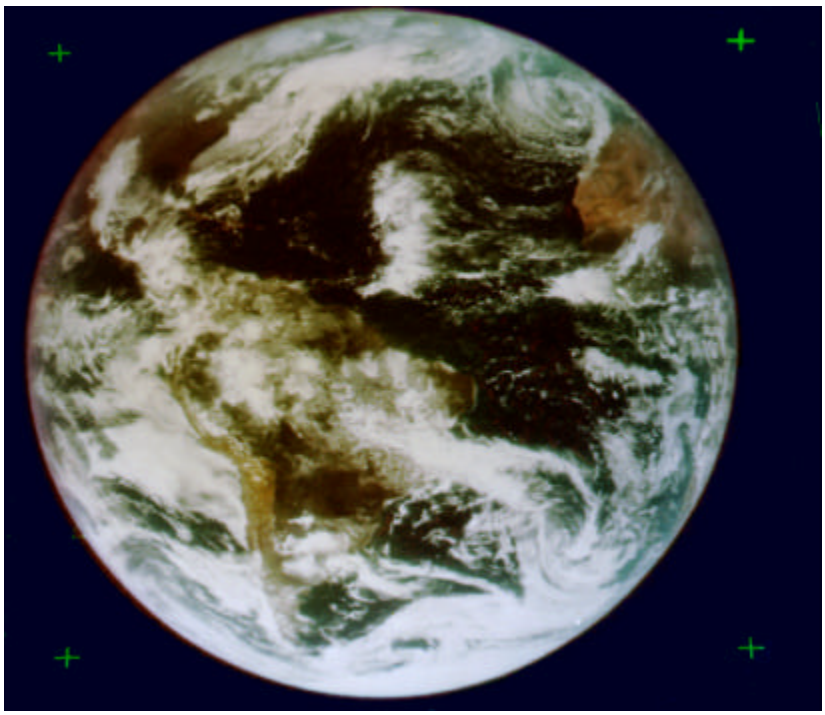

Figure 7-7. Earth in color from geosynchronous orbit - ATS-3

F GOES

1 Satellite and Sensor

The Geostationary Operational Environmental Satellite (GOES) mission provides the now-familiar weather pictures seen on newscasts worldwide. Each satellite in the series carries two major instruments, an imager and a sounder, which acquire high-resolution visible and infrared data, as well as temperature and moisture profiles of the atmosphere.

The GOES I-M system serves a region covering the central and eastern Pacific Ocean; North, Central, and South America; and the central and western Atlantic Ocean. Pacific coverage includes Hawaii and the Gulf of Alaska. This is accomplished by two satellites, GOES West located at 135 west longitude and GOES East at 75 west longitude. A common ground station, the CDA station located at Wallops, Virginia, supports the interface to both satellites.

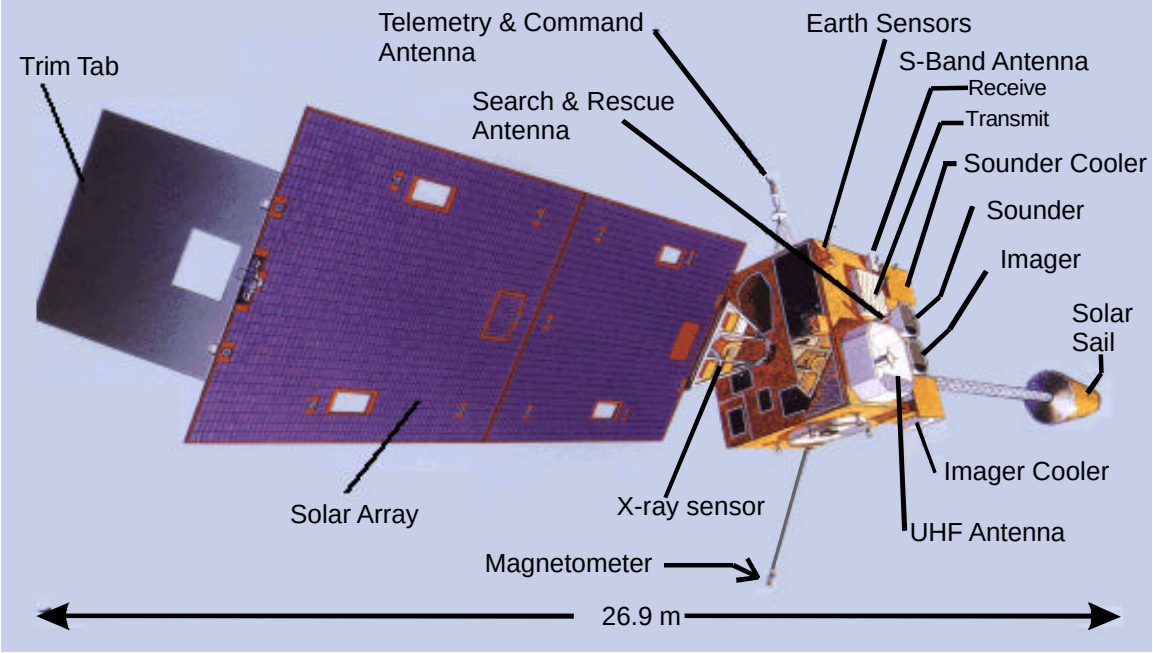

Figure 7-8. GOES

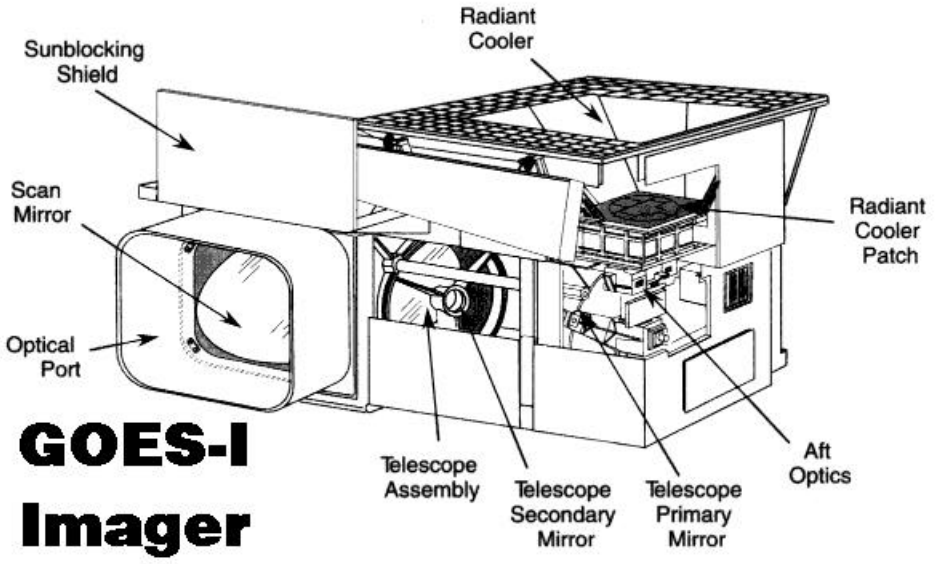

Figure 7-9

Figure 7-10. GOES-8 spectral response functions.

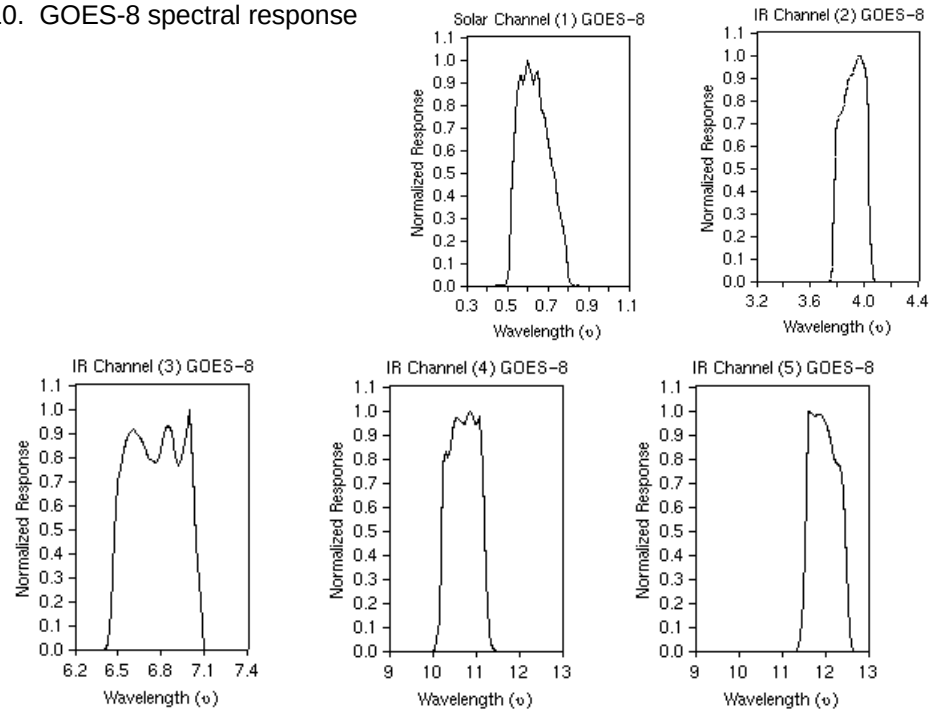

GOES 9 - 1930 UTC 4 April 1998
visible, 4 micron, 11 micron

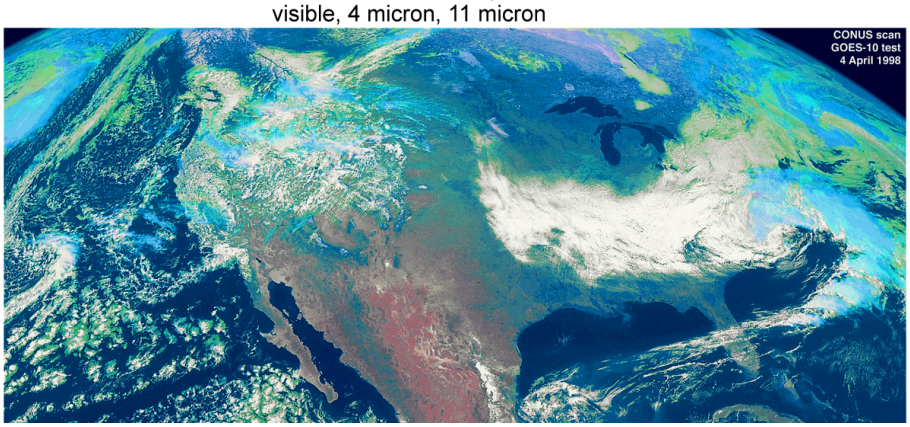

Figure 7-11 GOES vs NOAA : geosynchronous vs polar
Continuous view from geo - once every 15-30 minutes, 1 km resolution
Nadir view - worldwide coverage from polar orbiter.

2 Weather and storms - Hurricane Mitch

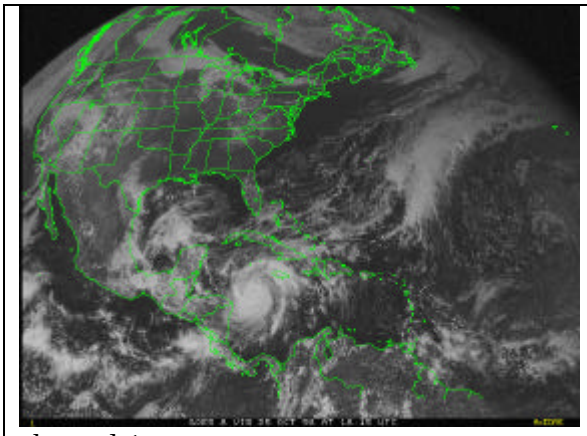

channel 1

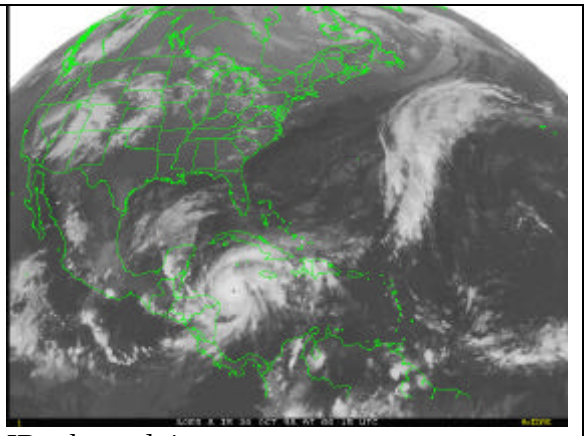

IR: channel 4

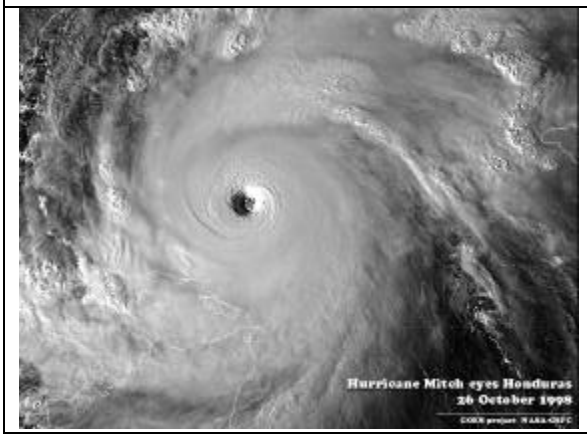

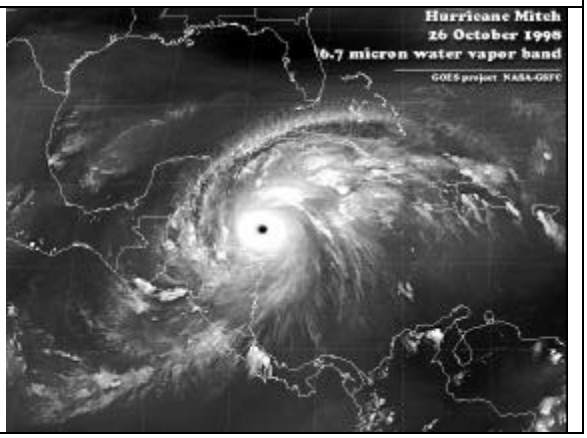

Figure 7-12 Weather

3 Volcanoes and ash clouds

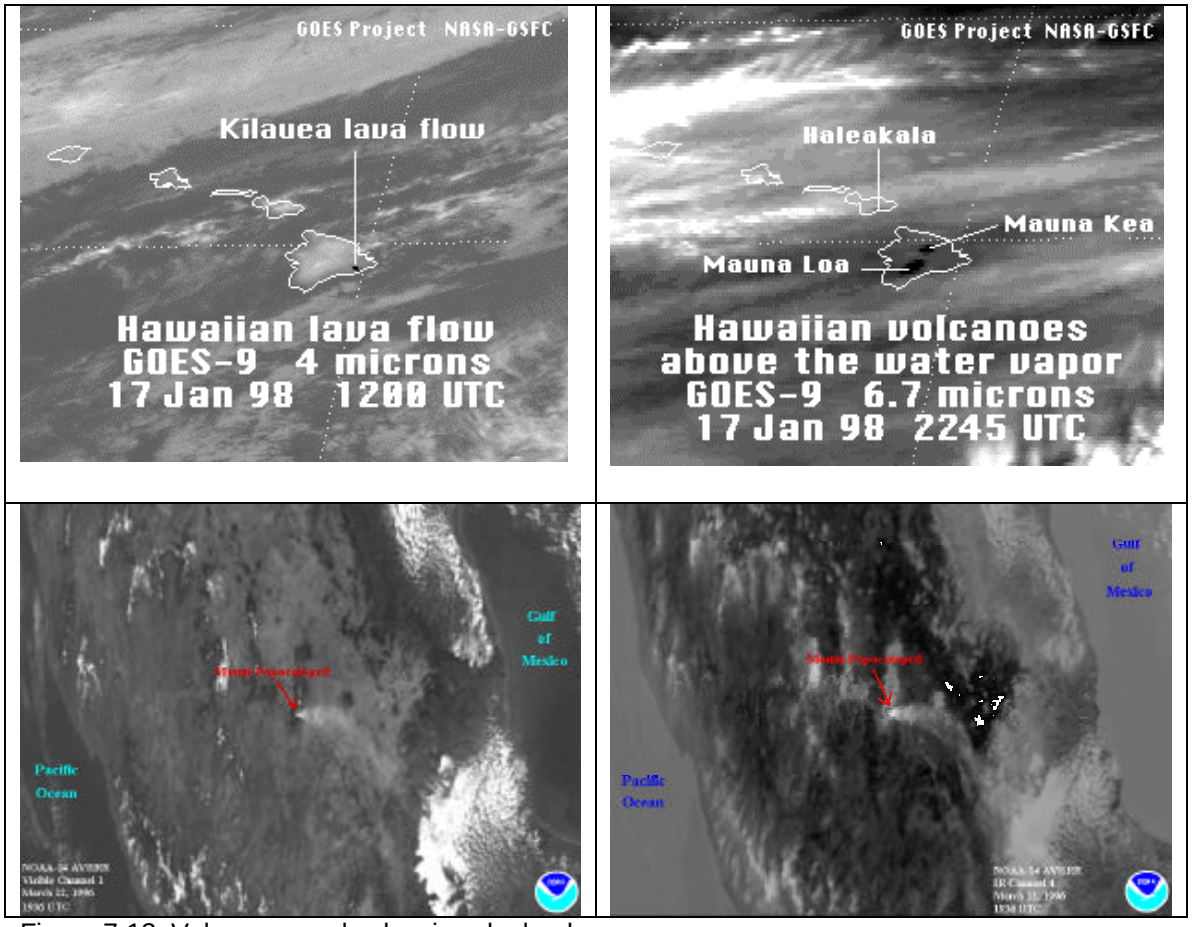

Figure 7-13. Volcanoes and volcanic ash clouds

The fact that the peaks of the Hawaiian volcanoes rise above the water vapor layer are a primary reason why they make good places for astronomical observatories. Volcanic ash clouds are a hazard for aviation, and are not easily detected by other means.

4 Shuttle launch - vapor trail, rocket

The GOES satellite makes a nice analogue for a missile warning satellite. The vapor trail is visible in the first trail (the white cloud you see from the ground). The hot, sub-pixel, target is visible in all 4 of the infrared channels. The long-wave channels (11, 12 μ) don't show very good contrast, because the earth is already bright at that wavelength. The highest contrast is in the 6.7 μ channel, because the atmospheric water vapor prevents the sensor from seeing the extensive ground clutter.

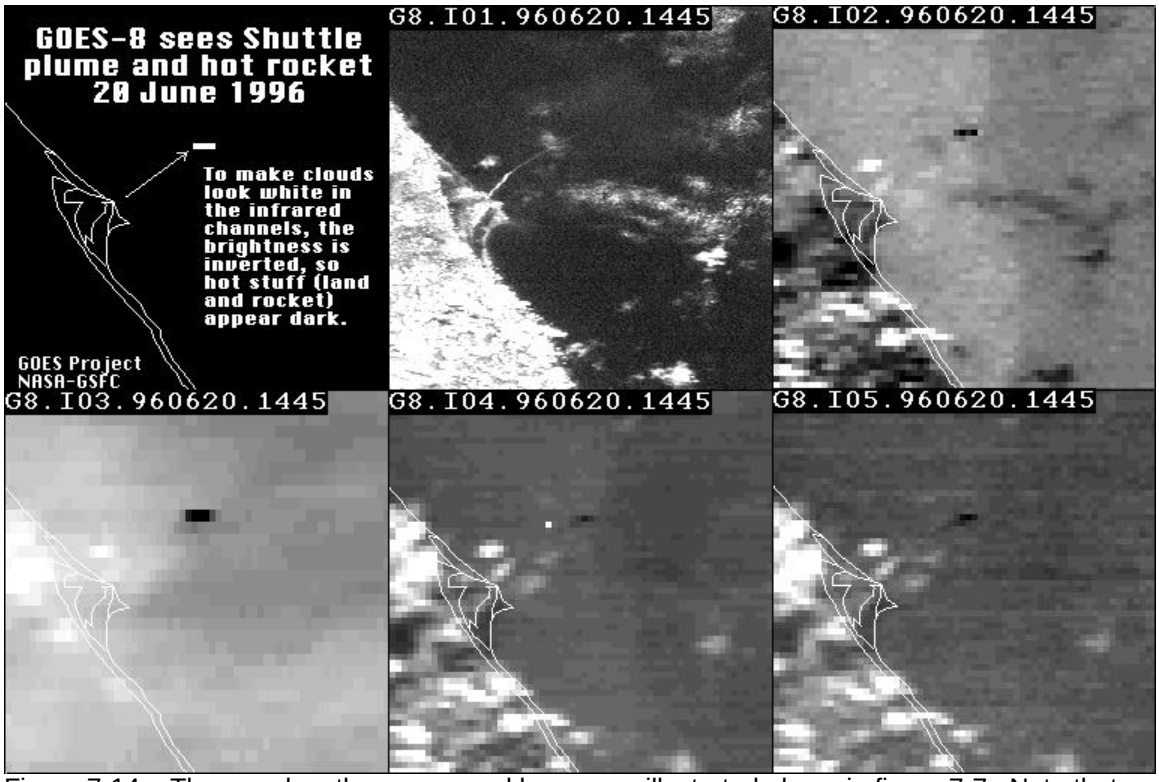

Figure 7-14. The wavelength ranges used here were illustrated above in figure 7-7. Note that the third frame, from the 6.7μ channel shows the greatest signal-to-background.

5 SEBASS - thermal spectral

G Problems

1. At what wavelength does the radiation peak for targets at 300 K ?
What is the ratio of the total power per unit area emitted by a person (300 K) and a hot vehicle (1000 K)?

2. What are the tradeoffs between using MWIR (3-5 μm) vs LWIR (8-13 μm)
Consider the radiated energy, the detector technology (cooling issues), Rayleigh Criteria concerns.

2. Of the materials in table 2, which will show the largest temperature fluctuation during a 24-hour heating/cooling cycle; which will show the smallest fluctuation?

This page intentionally left blank